Osteoarthritis and Cartilage 27 (2019) 1800–1810

Osteoarthritis and Cartilage

# Accelerated post traumatic osteoarthritis in a dual injury murine model

K. McCulloch †, C. Huesa †, L. Dunning †, G.J. Litherland †, R.J. Van 'T Hof ‡, J.C. Lockhart † ** [a], C.S. Goodyear § * [a]

† Institute of Biomedical & Environmental Health Research, University of the West of Scotland, Paisley, PA1 2BE, UK
‡ Institute of Ageing and Chronic Disease, University of Liverpool, WH Duncan Building, West Derby Street, Liverpool, L7 8TX, UK
§ Centre of Immunobiology, Institute of Infection, Immunity and Inflammation, College of Medical, Veterinary and Life Sciences, University of Glasgow, Glasgow, G12 8TA, United Kingdom

ARTICLE INFO

*Article history:*
Received 18 December 2018
Accepted 21 May 2019

*Keywords:*
Post-traumatic osteoarthritis
Osteophytes
Synovitis
Pain

SUMMARY

*Objective:* Joint injury involving destabilisation of the joint and damage to the articular cartilage (e.g., sports-related injury) can result in accelerated post-traumatic osteoarthritis (PTOA). Destabilised medial meniscotibial ligament (DMM) surgery is one of the most commonly used murine models and whilst it recapitulates Osteoarthritis (OA) pathology, it does not necessarily result in multi-tissue injury, as occurs in PTOA. We hypothesised that simultaneous cartilage damage and joint destabilisation would accelerate the onset of OA pathology.

*Methods:* OA was induced in C57BL/6 mice via (a) DMM, (b) microblade scratches of articular cartilage (CS) or (c) combined DMM and cartilage scratch (DCS). Mice were culled 7, 14 and 28 days post-surgery. Microcomputed tomography (μCT) and histology were used to monitor bone changes and inflammation. Dynamic weight bearing, an indirect measure of pain, was assessed on day 14.

*Results:* Osteophytogenesis analysis via μCT revealed that osteophytes were present in all groups at days 7 and 14 post-surgery. However, in DCS, osteophytes were visually larger and more numerous when compared with DMM and cartilage scratch (CS). Histological assessment of cartilage at day 14 and 28, revealed significantly greater damage in DCS compared with DMM and CS. Furthermore, a significant increase in synovitis was observed in DCS. Finally, at day 14 osteophyte numbers correlated with changes in dynamic weight bearing.

*Conclusion:* Joint destabilisation when combined with simultaneous cartilage injury accelerates joint deterioration, as seen in PTOA. Thus, DCS provides a novel and robust model for investigating multiple pathological hallmarks, including osteophytogenesis, cartilage damage, synovitis and OA-related pain.


## Introduction

Osteoarthritis (OA) is globally the most prevalent musculoskeletal disease.[1] OA is characterised by significant structural changes in joint tissues such as articular cartilage degradation, osteophyte formation (bony outgrowths), subchondral osteosclerosis, epiphyseal bone expansion, synovitis and pannus formation. Although OA is often associated with increasing age, an accelerated progression is recognised in individuals suffering previous (often sport-related) joint injury involving multi-tissue damage. Notably, 66% of patients presenting with articular surface damage in their joints progressed towards OA.[2,3] Furthermore, current data suggests that patients with chronic OA who suffered an earlier articular trauma are, upon diagnosis, >10 years younger than those patients with no history of joint injury.[4] Taken together, post-traumatic OA (PTOA), as characterised by accelerated joint degeneration, pain and dysfunction, accounts for ~12% of all OA cases.[5]

Lapine models used to investigate PTOA resulting from multi-tissue joint injury, usually involve traumatic rupture of the

* Address correspondence and reprint requests to: Prof. C.S. Goodyear, Sir Graeme Davies Building, 120 University Place, Glasgow, G12 8TA, Scotland, UK.
** Address correspondence and reprint requests to: Prof. J.C. Lockhart, Institute of Biomedical & Environmental Health Research, University of the West of Scotland, Paisley, PA1 2BE, UK.
*E-mail addresses:* John.Lockhart@uws.ac.uk (J.C. Lockhart), Carl.Goodyear@glasgow.ac.uk (C.S. Goodyear).
[a] Joint senior and corresponding authors.

https://doi.org/10.1016/j.joca.2019.05.027

anterior cruciate ligament (ACL) and damage of surrounding tissues including the meniscus via mechanical impact on the patellofemoral joint.[6–8] These have yielded valuable insight into PTOA progression, but involve relatively undefined and uncontrolled damage to various joint tissues. In comparison, surgically-induced murine models that develop OA-like pathology include the destabilised medial meniscotibial ligament (DMM) model and anterior cruciate ligament transection (ACLT) murine model. While both recapitulate features of OA pathology, these do not arise directly from an initial multi-tissue injury, as occurs in PTOA. This may be an important limitation, as increasing evidence suggests that joint tissue interactions may play a significant role in driving disease progression.[9–12] Alternative murine models include articular injection of agents that induce inflammation and/or tissue toxicity/damage, but questions remain as to how well these represent the joint damage seen in OA.[13] To better understand accelerated OA progression, what is needed is a murine model that combines joint destabilisation with defined/controlled joint tissue injury, and is accessible to genetic manipulation, while enabling comprehensive evaluation of disease-related changes in relevant joint tissues (e.g., cartilage, bone, meniscus). The present study is the first to present a dual injury murine model involving simultaneous cartilage damage and joint destabilisation, and was developed to test our focused hypothesis that concomitant cartilage damage and joint instability accelerates the onset of OA pathology as seen in PTOA.

## Methods

### *Animals*

Experiments were performed on 10 week old adult 22–28 g wild-type C57BL/6 male mice (Envigo, UK). Mice were housed at the University of Glasgow or University of the West of Scotland and maintained under standard animal husbandry conditions in accordance with UK home office regulations. All procedures were performed in accordance with UK Home Office Regulations, and with study approval by Animal Welfare Ethical Review Boards at the University of Glasgow and the University of the West of Scotland.

### *Induction of OA*

OA was induced by one operator (to minimise surgical variability) under aseptic conditions via (a) transection of the medial meniscotibial ligament (DMM)[14], (b) microblade scratches of articular cartilage [cartilage scratch (CS); Supplemental Fig. 1(A)] or (c) combined DMM and cartilage scratch (DCS) [Supplemental Fig. 1(B)]. Three CSes were made only to the superficial cartilage on the medial side of the tibia underneath the medial meniscotibial ligament (MMTL) using a single use size 11 microblade (Swann-Morton), as indicated in Supplemental Fig. 1. DMM was carried out prior to CSes in the DCS model, with all surgeries lasting 10 ± 2 min. Buprenorphine (Vetergesic; 30 μg intraperitoneally) was administered pre-operatively. 2% oxygen and 2% Isoflurane (Isoflurane Vet, Merial) was used to anaesthetise animals throughout the surgical procedures. Animals were maintained for 7, 14 and 28 days, with knee joints subsequently harvested for μCT and histological analysis. Sham operated joints of OA-induced mice were used as controls.

### *Microcomputed tomography (μCT)*

Knee joints were fixed in 4% paraformaldehyde solution for 24 h, then transferred to 70% EtOH and analysed by μCT to examine the calcified tissues using a Skyscan 1272 μCT scanner (Bruker, Belgium; 0.5 aluminium filter, 50 kV, 200 μA). Samples were scanned at voxel size 4.5 μm, 0.5° rotation angle for quantification, and 2 μm, 0.2° rotation angle for imaging [Fig. 2(A); Fig. 3(A)&(B)]. Scans were reconstructed in NRecon software (Bruker, Belgium). Osteophytes were identified in the resulting three-dimensional image stacks using CTvol software (Bruker, Belgium) and then number of osteophytes per joint counted. Osteophyte bone volume was measured by manually delineating the edge of osteophytes protruding from the subchondral plate as the region of interest (ROI) for analysis, and quantified for bone volume using CTan software (Bruker, Belgium). Subchondral bone was analysed by selecting a volume of interest (VOI) of 0.5 × 0.9 × 0.9 $mm^3$ in the centre of load in the medial and lateral tibial plateau.[15] ROIs (medial and lateral) delineating the trabecular structure within the tibial epiphysis were selected in the 2D coronal view of the stack to analyse the bone volume and microarchitecture using CTAn.

### *Histological assessment of cartilage damage and synovitis*

Joints were decalcified overnight (Formical 2000; Decal Chemical, New York, USA) and embedded in paraffin wax. Coronal sections (6 μm) were cut and then stained with haematoxylin, safranin-O/fast green. Using a validated scoring system[14] ranging from 0 (normal) to 6 (>80% loss of cartilage), severity of cartilage damage was assessed histologically on joints previously scanned for micro computed tomography (uCT). Two scorers blinded to the specimens, scored the medial tibial quadrant in 4–6 sections from each mouse. We did not include initial cartilage lesions inflicted by microblade scratches in both cartilage damage and DCS models in our scoring. Synovitis was assessed by two blinded scorers using a recently developed scoring system[16] which we modified from the original to focus only on pannus formation, synovial membrane thickening and sub-synovial hyperplasia. For both scoring systems, there was good agreement between scorers with intraclass correlation coefficient for cartilage scoring of 0.96 (95% CI 0.92 to 0.98), and synovitis scoring of 0.83; (95% CI 0.65 to 0.92).

### *dynamic weight bearing*

As an indirect measurement of pain, limb weight bearing was assessed in mice 14 days after surgery using the BioSeb Dynamic Weight Bearing (DWB) chamber (BioSeb, Marseilles, France). All animals were individually recorded for 5 min, 1 min of which was validated and subsequently analysed. The parameters examined were load on ipsilateral (injured) hind paw and load on front paws.

### *Statistical analysis*

Prism 6 (Graphpad) was used to perform statistical analysis. For normally distributed data, analysis involved one-way analysis of variance (ANOVA) and multiple comparisons using Bonferroni correction. Student *t*-tests were also used. Data not normally distributed was analysed by Kruskal–Wallis one-way ANOVA and multiple comparisons using Dunn's corrections. Linear regression curves were generated and Spearman's correlation coefficient ($\rho$) was used to assess strength of relationship. *P* values less than 0.05 were considered significant.

## Results

### *Accelerated osteophyte development after dual injury*

Evaluation of osteophyte formation at an early timepoint (7 days post-surgery) revealed that although osteophytes could be detected in some mice within each of the experimental groups [Fig. 1(A)

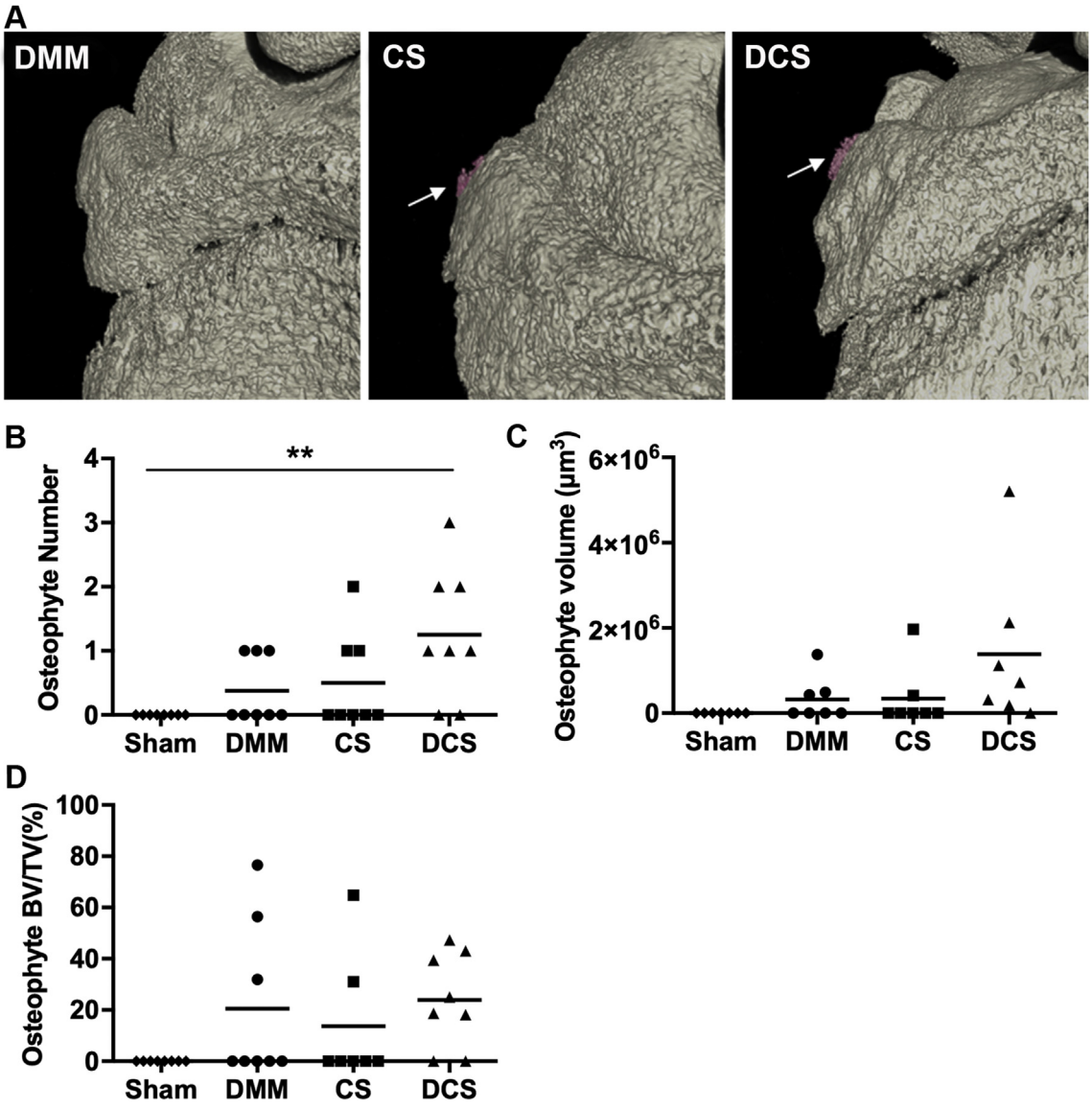


**Fig. 1. Osteophyte development 7 days post-surgery.** (A) Three-dimensional microCT (μCT) imaging of developing osteophytes (arrows) following Destabilised medial meniscotibial ligament (DMM); cartilage damage; and DMM and cartilage scratch (DCS) in C57BL/6 mice. Quantitative data showing (B) osteophyte number (C) osteophyte tissue volume and (D) % of bone within osteophyte (bone volume/tissue volume, BV/TV) present in each sample within each surgical group. $^{**}P < 0.01$; $n = 8$. DMM; cartilage scratch (CS); DCS.

and (B)] there was an increase in detectable osteophytes in the DCS model. Notably, in the DCS group 6 out of 8 mice had observable osteophytes whilst only 3 out of 8 mice in the DMM and CS showed signs of osteophytogenesis [Fig. 1(B)]. Moreover, at day 7 the osteophytes in the DCS group were quantifiably larger in size [Fig. 1(C)] and in some mice more numerous [Fig. 1(B)]. In comparison, the DMM group osteophytes were reduced in both number and volume [Fig. 1(B) and (C)]. Analysis of osteophyte BV/TV at day 7 did not show any detectable increased bone volume across any of the three experimental groups [Fig. 1(D)].

To determine how these osteophytes develop over time in these models, we investigated osteophyte morphology and structural characteristics at day 14. In the DMM group, arboreal-like osteophytes were observable in 6 out of 8 mice, whilst in the CS and DCS mice, 100% of mice exhibited osteophytes [Fig. 2(A),(B) and (C)]. Importantly, at this time point, DCS mice had significantly more osteophytes than the DMM and CS groups [Fig. 2(C)], with a minimum of two observable osteophytes. However, 5 out of 8 DCS mice presented with 3 osteophytes per joint [Fig. 2(C)]. In comparison, both DMM and CS alone animals presented a maximum of two osteophytes, which were only seen in 3 out of 8 of mice in each group [Fig. 2(C)]. Both CS and DCS groups exhibited significantly larger osteophyte volume compared to DMM and sham groups [Fig. 2(C)]. However, the percentage of bone volume within these osteophytes did not differ significantly between experimental model groups [Fig. 2(E)].

### *Dual injury promotes subchondral osteosclerosis*

Analysis was undertaken to investigate the impact of DMM, CS and DCS on the subchondral bone. At day 7, μCT analysis showed an increase of subchondral osteosclerosis in all 3 OA models when compared with sham controls [Fig. 3(A)]. At day 14 the level of subchondral osteosclerosis in the CS group remained constant, however there was a further increase in subchondral BV/TV in both DMM and DCS models; possibly due to joint instability and

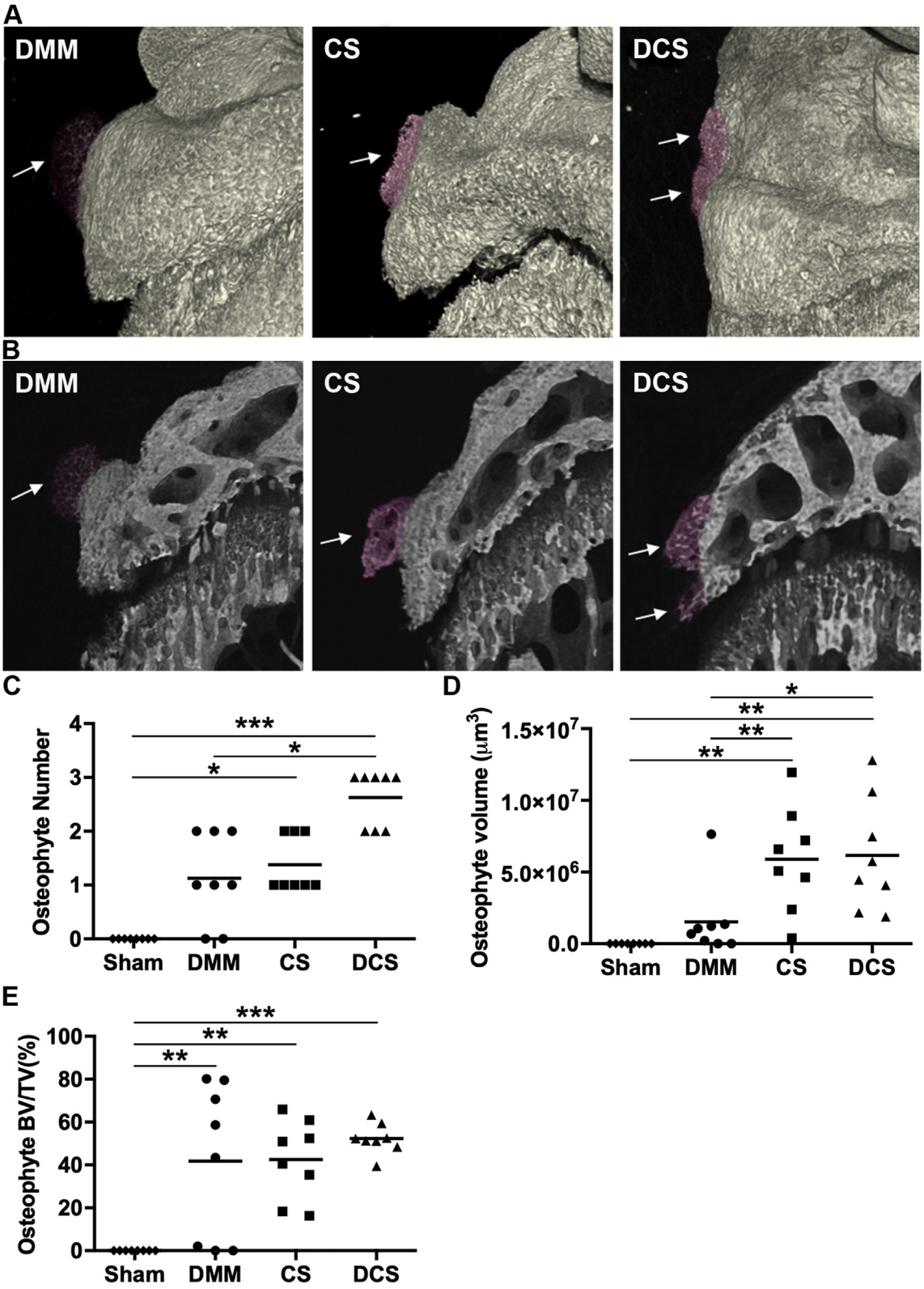


**Fig. 2. Osteophyte development 14 days post-surgery.** (A) Three-dimensional μCT imaging of developing osteophytes (arrows) following DMM; cartilage damage; and DCS in C57BL/6 mice, and (B) corresponding sagittal plane images. Quantitative data showing accelerated osteophytogenesis in the DCS model exhibited by (C) osteophyte number (Kruskal–Wallis with Dunns multiple comparison); (D) total osteophyte volume (Student's *t*-test), (E) % of bone present within osteophytes. $^{*}P < 0.05$; $^{**}P < 0.01$; $^{***}P < 0.001$; $n = 8$. DMM, DMM; CS; DCS.

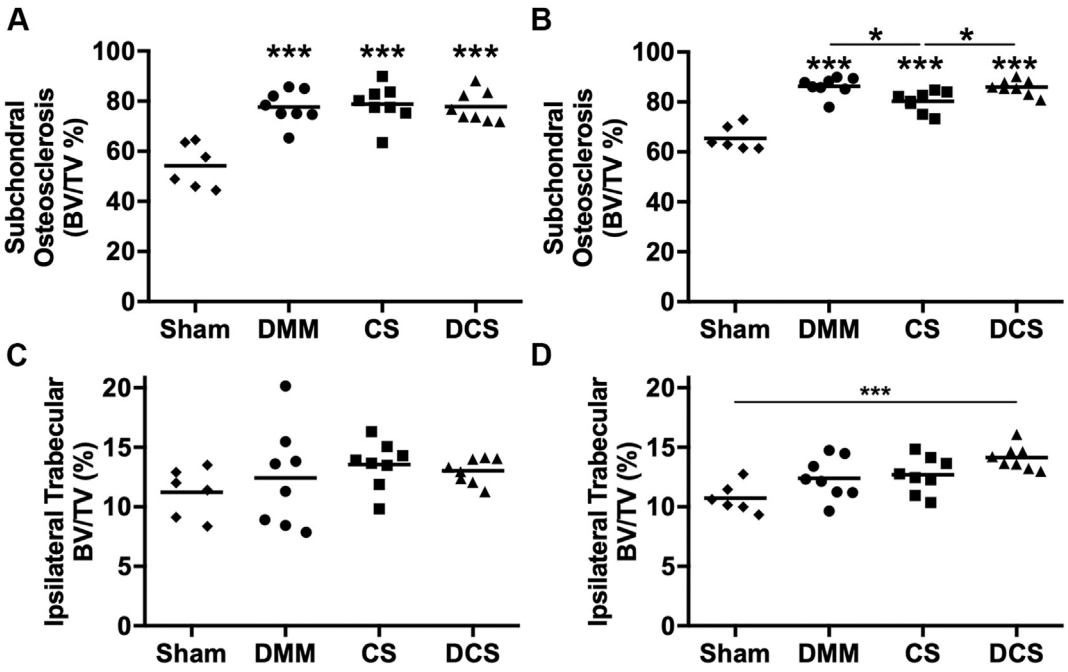


**Fig. 3. Subchondral osteosclerosis is evident at day 7 post-surgery with increased trabecular bone volume at day 14.** (A) Day 7 post-surgery subchondral osteosclerosis. (B) Day 14 post-surgery subchondral osteosclerosis. (C) Changes in trabecular bone volume/tissue volume (BV/TV) at day 7. (D) Trabecular BV/TV changes at day 14 post-surgery. $^{*}P < 0.05$; $^{**}P < 0.01$; $^{***}P < 0.001$ (without bar is cf. Sham); $n = 6–8$. DMM; CS; DCS.

increased biomechanical loading [Fig. 3(B)]. There were no observable differences in metaphyseal trabecular bone in the ipsilateral (injured) leg at day 7 post-surgery [Fig. 3(C)]. However, at day 14, DCS mice exhibited a significant increase in trabecular BV/TV in the injured leg [Fig. 3(D)].

*Dual injury increases cartilage degradation and synovitis*

While cartilage damage and/or synovitis were not normally detectable at day 14 post-induction, we sought to investigate whether these might emerge in the DCS model at this early timepoint as an indicator of accelerated PTOA. Histological analysis of the medial compartment of the knee joint at 14 days following DMM, CS or DCS surgery was performed. Over and above the initial scratch-induced cartilage damage, we found significant further cartilage degradation in the DCS model on the tibia when compared with DMM and CS models [Fig. 4(A)–(D)]. Consistent with this finding we also observed increased cartilage degradation on the femur in the DCS model compared with DMM and CS models [Fig. 4(E)]. Furthermore, although there was observable synovitis in the DMM and CS groups, there was a significant increase in synovitis in the DCS model [Fig. 4(F)]. Correlation analysis revealed a strong relationship between cartilage damage and synovitis levels ($\rho = 0.77$, $P = 0.0004$) [Fig. 4(G)], as well as between cartilage damage and osteophyte number ($\rho = 0.59$, $P = 0.003$) [Fig. 4(H)]. Synovitis also positively correlated with the number of osteophytes present ($\rho = 0.49$, $P = 0.02$) [Fig. 4I]. In addition, we sought to investigate if accelerated cartilage damage and synovitis in the DCS model persists at 28 days post-surgery [Fig. 5(A)–(C)]. Notably, both increased cartilage damage in the medial tibia and femur [Fig. 5(D) and (E)] and synovitis [Fig. 5(F)] was observed in the DCS group at 28 days post-surgery. Moreover, we also observed remodelling of the cartilage at day 28 in the DCS model [Fig. 5(C)], a feature linked with increasing severity of OA pathology.[17] Taken together this indicates that DMM combined with CS promotes an acute inflammatory environment with progressive and accelerated cartilage degradation, remodelling and enhanced osteophytogenesis

*Osteophyte number and cartilage damage correlate with pain-related behaviour*

Prior work by Huesa *et al.* has shown that DWB can be used to monitor pain-related behaviour.[18] Fourteen days post-surgery, mice in the DCS group demonstrated a significant loss of loading on their ipsilateral (injured) leg when compared with DMM alone [Fig. 6(A)]. No significance was observed in load on the contralateral (non-injured) hind limb between all groups. Consistent with this, mice in the DCS group also demonstrated a significant increase in front paw load compared with the other models [Fig. 6(B)], indicating an increase in OA-related pain. Importantly, there was a strong positive correlation between osteophyte number and front paw load at this time point ($\rho = 0.65$, $P = 0.0004$) [Fig. 6(C)]. Suggesting that the severity of OA-related pain may be related to the extent of osteophytogenesis. As we observed a positive correlation between osteophyte number and both cartilage damage and synovitis, we further investigated these parameters in relation to OA-pain related behaviour: however, neither cartilage damage nor synovitis exhibited a significant correlation with increase front paw load ($\rho = 0.35$, $P = 0.09$ and $\rho = 0.28$, $P = 0.19$ respectively).

## Discussion

Trauma to the joint is known to promote early osteoarthritis, but the mechanisms for accelerated disease are not well understood. This study presents a novel dual injury murine model to address the important question of whether concomitant joint destabilisation and defined cartilage damage leads to early OA characterised by progressive cartilage destruction, osteophytogenesis, synovitis and pain.

Critical to model selection and/or development, is the specific research hypothesis being addressed; and how translatable these

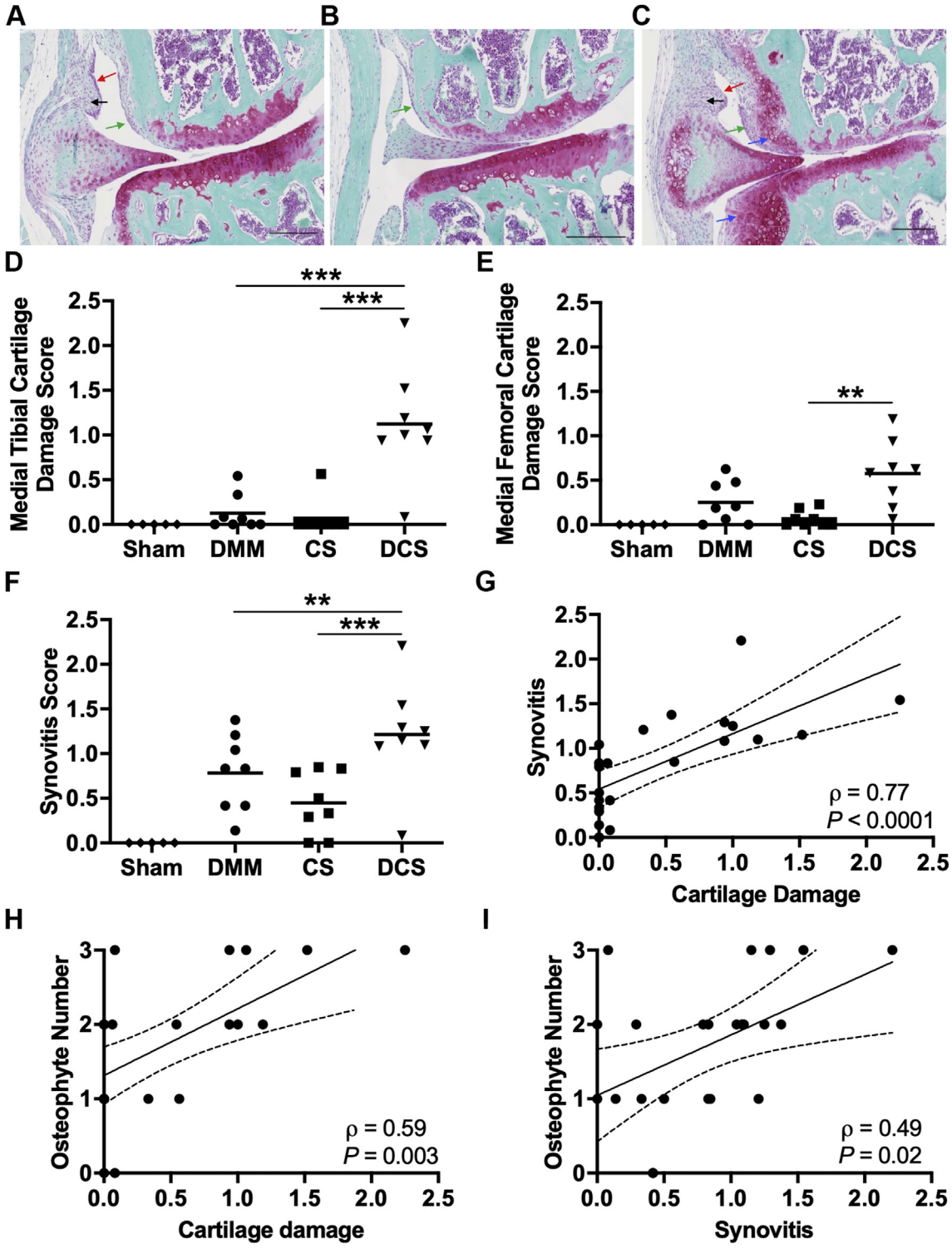


**Fig. 4. Cartilage degradation and synovitis 14 days post-surgery.** Histological appearance of the medial compartment of the knee joint 14 days following (A) DMM (B) Cartilage damage or (C) DCS, showing pannus formation (green arrow), synovial hyperplasia (red arrow), sub-synovial hyperplasia (black arrow) and Subchondral bone/osteophyte formation (blue arrow). Scale bar = 200 μm. Cartilage damage scores for the (D) medial tibial and (E) medial femur, and (F) Synovitis scores in mice following DMM, cartilage damage or DCS surgery at 14 days post-surgery. Correlation curves depicting significant correlations between (G) cartilage damage and synovitis; (H) osteophyte number and cartilage damage; (I) osteophyte number and synovitis. 95% confidence intervals are indicated by dotted lines. $^{*}P < 0.05$; $^{**}P < 0.01$; $^{***}P < 0.001$; $n = 8$. DMM; CS; DCS.

findings are to human OA. There are various well-established and widely used experimental models of OA across a range of species. While none are ideal in modelling human disease, Little and colleages have identified preferred characteristics, which include recapitulating human joint disease in a manner amenable for measurement and monitoring, and within a reasonable time frame.[19] Model types range from surgicial induction and traumatic injury, to chemical induction methods, each with their strengths

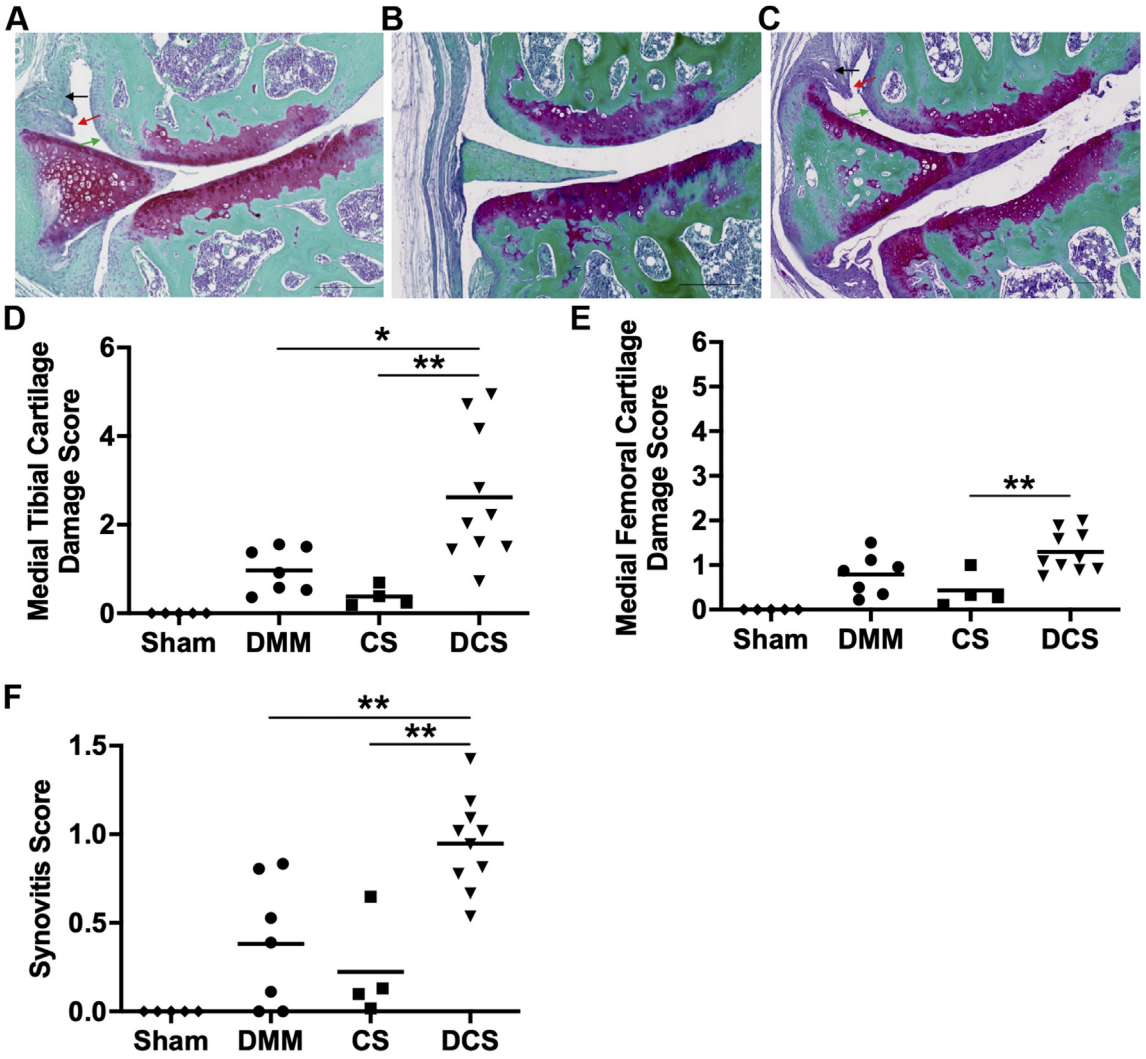


**Fig. 5. Cartilage degradation and synovitis 28 days post-surgery.** Histological appearance of the medial compartment of the knee joint 28 days following (A) DMM (B) cartilage damage or (C) DCS, showing pannus formation (green arrow), synovial hyperplasia (red arrow), sub-synovial hyperplasia (black arrow) and subchondral bone/osteophyte formation (blue arrow). Scale bar = 200 μm. Cartilage damage scores for the (D) medial tibial and (E) medial femur, and (F) synovitis scores in mice following DMM, cartilage damage or DCS surgery at 14 days post-surgery. $^{*}P < 0.05$; $^{**}P < 0.01$. DMM, DMM; CS, CS; DCS, DCS.

and limitations. For example, blunt trauma results in relatively undefined multi-tissue injuries, surgical approaches risk surgical artefact whilst chemical approaches such as intra-articular injection of monoiodoacetate (MIA) likely evoke joint changes by mechanisms different from those underpinning OA.

Murine models are important tools for research on various human diseases, and for OA, one of the most widely used is the DMM surgical induction model generated by Glasson *et al.*.[14] This induces joint instability and recapitulates the cartilage damage, osteosclerosis, osteophytogenesis and pain that characterise OA in humans, although is technically demanding with respect to surgical skill and need for aseptic conditions. Nevertheless, an experienced researcher can achieve good reproducibility with minimal surgical artefact, and thus we consider DMM to be a robust model in our OA research programme. However, DMM does not reproduce the acute trauma-induced damage to surrounding soft tissue (including cartilage) that is observed in human sport-related injuries.[20,21] PTOA is characterised by accelerated pathology post-injury, and there is a recognised subcohort of OA patients with symptoms limiting life-style at an earlier time point than normally seen. While this is likely to be a consequence of the synergistic interaction of injury to multiple joint tissues, the exact mechanisms driving this accelerated disease progression are not fully understood. In the context of traumatic injury, altered joint loading and initial cartilage damage as a consequence of meniscal damage has been linked with OA development.[22] Rabbit ACL rupture models involving blunt impact trauma are available to study PTOA.[7,8,23] Whilst these models can imitate and reproduce multi-tissue damage similar to that of human knee joint impact traumas, they are limited in not being able to target and confine this trauma specifically to defined tissues within the joint in a reproducible fashion. To this end we have developed a novel dual-injury murine model specific for investigation of OA arising from simulataneous cartilage damage and joint destabilisation. Our DCS procedure now enables generation of a controlled multi-tissue injury murine model mimicking significant trauma to a healthy knee. The DCS model is thus highly relevant to human disease, offering significant potential in meeting a currently unmet scientific need for a model that more accurately represents the subcohort of young otherwise healthy individuals suffering accelerated PTOA resulting from sporting injuries. Such injuries involve simultaneous damage to various joint tissues, including ligaments, bone and cartilage. With this model we

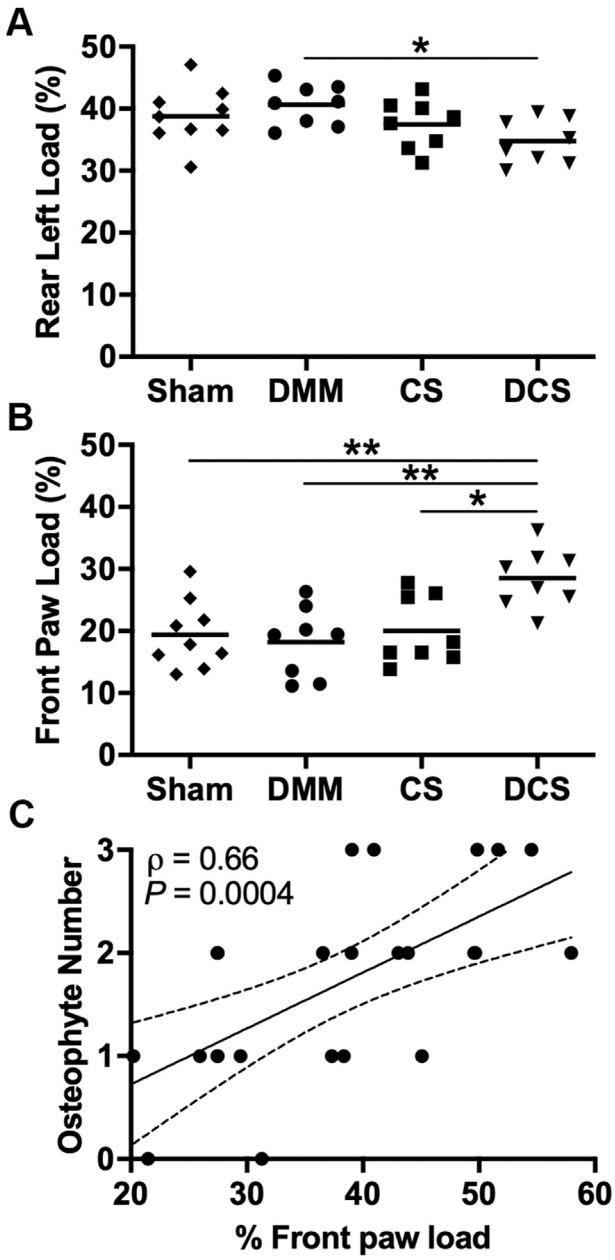


**Fig. 6. Increased pain-related behaviour correlates with osteophyte number and cartilage damage at day 14 post-surgery.** Dynamic weight bearing measurements of the (A) ipsilateral (injured) paw and (B) front paw load for mice following DMM, cartilage damage or DCS surgery at 14 days post-surgery. (C) Correlation curves depicting significant correlation between front paw load and osteophyte number across the models. 95% confidence intervals are indicated by dotted lines. $^{*}P < 0.05$; $^{**}P < 0.01$; $^{***}P < 0.001$; $n = 8$. DMM, DMM; CS, CS; DCS, DCS.

observed accelerated PTOA via combination of defined cartilage micro-lesions (Supplemental Fig. 1(D)) with altered loading due to destabilisation of the medial meniscus, allowing us to investigate mechanisms known to be key OA triggers in human disease.

Osteophyte formation is believed to be a response mechanism triggered by a loading imbalance within the joint, expanding the surface area of the tibial plateau to better support the alteration in biomechanical loading.[24,25] We have previously shown DMM alone can induce osteophytogenesis as early as day seven post-surgery in C57BL/6 mice.[18] This is consistent with the present study, in which we report the presence of small osteophytes, low in number, in the DMM model at day seven [Fig. 1(B) and (C)]. Few, small osteophytes were also present in the CS model at day 7 [Fig. 1(A) and (B)]. However, the DCS model presented with quantifiably larger, and in most mice, more numerous osteophyte formation at day 7 [Fig. 1(A) and (B)]. These data would suggest dual trauma consisting of cartilage damage and joint destabilisation can accelerate the formation of osteophytes as early as 7 days post-injury. Previous studies have reported that secondary osteophyte growth is initiated by cartilage damage,[26–28] however the factors influencing the formation and growth of osteophytes are poorly defined. Cartilage lesions have been associated with the formation of larger osteophytes,[29] supporting our day 14 findings of both cartilage damage and DCS models presenting with larger, more numerous osteophytes compared with the DMM model [Fig. 2(C) and (D)], where no initial cartilage damage was induced. This provides evidence that osteophytogenesis is accelerated by cartilage damage when combined with simultaneous joint loading imbalance. The specific site of cartilage damage may itself alter the type of pathologic outcome. Our study focussed on cartilage damage within the medial compartment however, there could be value in future studies focussing on the impact of cartilage damage on alternative sites (i.e., non-weight-bearing areas of cartilage) to determine how this affects pathologic outcome. Whilst the DCS model was developed to test a specific hypothesis, it has considerable potential to extend beyond OA, to investigation of osteophytogenesis in various pathological scenarios. Examples include ankylosing spondylitis and degenerative disk disease. Additionally, the study of osteophytogenesis could provide a controlled tool to investigate the initiation of endochondral ossification.

Another prominent feature of OA is the development of osteosclerosis in subchondral bone. When the cartilage becomes damaged there is an increased transfer in load to the subchondral bone,[30] as well as the release of inflammatory and osteoclast stimulation factors, which can lead to an increase in bone remodelling.[31,32] Osteosclerosis was measured as an increase in bone volume (% BV/TV) in the medial subchondral region of the tibia. At both 7 and 14 days post-surgery, all disease model groups exhibited evident osteosclerosis in the loaded medial compartment of the joint, where the destabilisation and/or cartilage damage was induced. After the initial increase at day 7, osteosclerosis in the CS model remained relatively constant at 14 days, whereas both the DMM and DCS groups significantly increased, indicating altered biomechanical load plays a key role in the development of osteosclerosis. Furman *et al.* showed that intra-articular fractures led to subchondral bone thickening and sclerosis of the knee in C57BL/6 mice.[33]

The observation that cartilage degradation is more extensive and progressive in the DCS model than either of the other models, suggests that interactions arising from the dual injury exacerbates cartilage breakdown. Trauma to the articular cartilage results in the activation of genes encoding for morphogens and the secretion of soluble inflammatory mediators into the joint cavity.[34–37] The formation of microcracks and increased vascularisation associated with abnormal bone remodelling in joints during OA facilitate molecular transport between cartilage and bone[9], therefore soluble inflammatory mediators present in the joint cavity as a result of cartilage damage and joint destabilisation may potentiate further cartilage destruction/bone remodelling, thus accelerating joint pathology in PTOA. Interestingly, we observed a significant correlation between cartilage damage and osteophyte number [Fig. 4(H)], raising the intriguing possibility that soluble factors secreted by the damaged cartilage may contribute to accelerated osteophytogenesis. Cartilage damage also exhibited a positive correlation with synovitis [Fig. 4(G)] suggesting a link with inflammatory factors.

While traditionally considered a ‘wear and tear’ disease, inflammation is increasingly recognised to have a role in

degenerative changes occurring during OA pathogenesis[38]. Histological features consistent with synovitis have been observed in synovium from OA patients[39–42] as well as expression of pro-inflammatory cytokines,[41,42] and more recently we have reported considerable heterogeneity of various inflammatory indices in OA synovia.[43] Indeed knee arthrocopic studies of OA patients found synovial inflammation to be associated with OA structural severity,[44] whilst another study reported that serum C-reactive protein levels in early osteoarthritis predicted likely progressive disease;[45] c-reactive protein (CRP) also correlates significantly with disease joint count and radiographic score in OA.[46] Whilst the DMM model does recaptitulate many of the characteristic features of OA, it is generally considered a non-inflammatory model.[47] Our study, however, supported by previous findings,[16] detected histologically the presence of synovitis at 14 days post-surgery. Nevertheless, given the low-level nature of this synovitis, DMM is not the model of choice for investigation of inflammation in OA joints. While the MIA model evokes joint inflammation,[48] this inflammatory response is not intiated in a manner resembling that of OA. Our DCS model yielded a significant and consistently higher level of synovitis than seen in either the DMM or CS models and, similarly to cartilage degradation, synovitis was positively correlated with increased osteophyte number [Fig. 4I]. Thus DCS presents value in enabling mechanistic interrogation of the putative contribution of synovitis to OA pathogenesis.

Pain is one of the most common and physically limiting symptoms of OA, however the origin of this pain is still poorly understood. DWB presents a behavioural non-invasive means of assessing pain, although other factors (e.g., mechanical impediment) may influence the observed changes. Ipsilateral (injured) hind paw and front paw loading were analysed. There was a significant decrease in injured hind paw load with a corresponding increase in load on the front paws in the DCS model compared with all other groups [Fig. 6(A) and (B)], suggesting the combination of cartilage damage and DMM enhances pain-associated pathology. There have been conflicting studies regarding the relationship between pain and osteophytes in OA. One previous study presented a significant correlation between knee joint pain in OA patients with osteophytes present in the medial tibial condyle.[49] However, more recently, Sengupta *et al.* challenged this finding by reporting that the presence of high-signal osteophytes detected on magnetic resonance imaging (MRI) were not associated with pain or pain severity.[50] Our data demonstrates a significant and strong positive correlation between osteophyte number and front paw load at 14 days post-surgery [Fig. 6(C)]. Synovitis is known to lead to heightened pain sensitivity in knee OA[51] and we therefore elected to further explore this finding in relation to pain-associated behaviour in the DCS model. We did not observe a significant correlation between front paw load and synovitis or an increase in cartilage degradation. The association of osteophytogenesis, cartilage damage, synovitis and pain implicates a causal relationship, and this merits future research to define the nature of any such relationships; this may help identify possible molecular mechanisms driving osteophyte formation, as well as joint pain.

We conclude that the concomitant joint instability and cartilage injury that typify knee joint traumatic injury predispose to accelerated OA progression. To establish this we developed and validated a murine model of acute trauma involving simultaneous controlled damage to multiple joint tissues. This robustly mimicked the accelerated OA pathogenesis observed in otherwise normal individuals with PTOA, as characterised by osteosclerosis and (compared with DMM) enhanced cartilage degradation, synovial inflammation, osteophytogenesis and pain. Importantly, this model also provides a valuable research tool for investigating osteophytogenesis in various contexts, as the DCS model generates an accelerated and more extensive formation of osteophytes at an early time-point. The reproducible synovitis associated with this model also presents means to elucidate the role of synovitis in OA pathology. Similarly, the enhanced pain-related behaviour in DCS provides a robust model for *in vivo* investigation of joint pain.

## Author contributions

Conceived and designed the experiments: KM, CH, JCL, CSG. Performed the experiments: KM, CH, LD. Analysed the data: KM, CH, LD, GL, RJvTH, JCL, CSG.; wrote manuscript: KM, CH, JCL,CSG.

## Competing interests

The authors declare no competing financial interests.

## Acknowledgements

This work was supported by a Programme Grant from Versus Arthritis (Grant #20199) and a PhD studentship from the University of West of Scotland. We would also like to thank Gemma Charlesworth and Mandie Prior (University of Liverpool) for their assistance with processing of bone tissue, immunhistochemistry and microCT.

## Supplementary data

Supplementary data to this article can be found online at https://doi.org/10.1016/j.joca.2019.05.027.

## References

1. Brooks PM. The burden of musculoskeletal disease–a global perspective. Clin Rheumatol 2006;25(6):778–81.
2. Curl WW, Krome J, Gordon ES, Rushing J, Smith BP, Poehling GG. Cartilage injuries: a review of 31,516 knee arthroscopies. Arthrosc J Arthrosc Relat Surg 1997;13(4):456–60.
3. Hjelle K, Solheim E, Strand T, Muri R, Brittberg M. Articular cartilage defects in 1,000 knee arthroscopies. Arthrosc J Arthrosc Relat Surg 2002;18(7):730–4.
4. Punzi L, Galozzi P, Luisetto R, Favero M, Ramonda R, Oliviero F, *et al.* Post-traumatic arthritis: overview on pathogenic mechanisms and role of inflammation. RMD open 2016;2(2). e000279-e.
5. Buckwalter JA. Sports, joint injury, and posttraumatic osteoarthritis. J Orthop Sport Phys Ther 2003;33(10):578–88.
6. Christiansen BA, Guilak F, Lockwood KA, Olson SA, Pitsillides AA, Sandell LJ, *et al.* Non-invasive mouse models of post-traumatic osteoarthritis. Osteoarthritis Cartilage 2015;23(10):1627–38.
7. Fischenich KM, Button KD, Coatney GA, Fajardo RS, Leikert KM, Haut RC, *et al.* Chronic changes in the articular cartilage and meniscus following traumatic impact to the lapine knee. J Biomech 2015;48(2):246–53.
8. Fischenich KM, Pauly HM, Button KD, Fajardo RS, DeCamp CE, Haut RC, *et al.* A study of acute and chronic tissue changes in surgical and traumatically-induced experimental models of knee joint injury using magnetic resonance imaging and micro-computed tomography. Osteoarthritis Cartilage 2017;25(4):561–9.
9. Yuan XL, Meng HY, Wang YC, Peng J, Guo QY, Wang AY, *et al.* Bone-cartilage interface crosstalk in osteoarthritis: potential pathways and future therapeutic strategies. Osteoarthritis Cartilage 2014;22(8):1077–89.

10. Findlay DM, Kuliwaba JS. Bone-cartilage crosstalk: a conversation for understanding osteoarthritis. Bone Res 2016;4:16028.
11. Macchi V, Stocco E, Stecco C, Belluzzi E, Favero M, Porzionato A, *et al*. The infrapatellar fat pad and the synovial membrane: an anatomo-functional unit. J Anat 2018;233(2):146–54.
12. Miyaki S, Lotz MK. Extracellular vesicles in cartilage homeostasis and osteoarthritis. Curr Opin Rheumatol 2018;30(1):129–35.
13. Teeple E, Jay GD, Elsaid KA, Fleming BC. Animal models of osteoarthritis: challenges of model selection and analysis. AAPS J 2013;15(2):438–46.
14. Glasson SS, Blanchet TJ, Morris EA. The surgical destabilization of the medial meniscus (DMM) model of osteoarthritis in the 129/SvEv mouse. Osteoarthritis Cartilage 2007;15(9):1061–9.
15. Das Neves Borges P, Forte AE, Vincent TL, Dini D, Marenzana M. Rapid, automated imaging of mouse articular cartilage by microCT for early detection of osteoarthritis and finite element modelling of joint mechanics. Osteoarthritis Cartilage 2014;22(10):1419–28.
16. Jackson MT, Moradi B, Zaki S, Smith MM, McCracken S, Smith SM, *et al*. Depletion of protease-activated receptor 2 but not protease-activated receptor 1 may confer protection against osteoarthritis in mice through extracartilaginous mechanisms. Arthritis Rheumatol (Hoboken, NJ) 2014;66(12):3337–48.
17. Pufe T, Petersen W, Tillmann B, Mentlein R. The splice variants VEGF121 and VEGF189 of the angiogenic peptide vascular endothelial growth factor are expressed in osteoarthritic cartilage. Arthritis Rheum 2001;44(5):1082–8.
18. Huesa C, Ortiz AC, Dunning L, McGavin L, Bennett L, McIntosh K, *et al*. Proteinase-activated receptor 2 modulates OA-related pain, cartilage and bone pathology. Ann Rheum Dis 2016;75(11):1989–97.
19. Little CB, Smith MM. Animal models of osteoarthritis. Curr Rheumatol Rev 2008;4(3):175–82.
20. Isaac DI, Meyer EG, Haut RC. Development of a traumatic anterior cruciate ligament and meniscal rupture model with a pilot in vivo study. J Biomech Eng 2010;132(6):064501–4.
21. Rosen MA, Jackson DW, Berger PE. Occult osseous lesions documented by magnetic resonance imaging associated with anterior cruciate ligament ruptures. Arthroscopy 1991;7(1):45–51.
22. Englund M, Roos EM, Lohmander LS. Impact of type of meniscal tear on radiographic and symptomatic knee osteoarthritis: a sixteen-year followup of meniscectomy with matched controls. Arthritis Rheum 2003;48(8):2178–87.
23. Ewers BJ, Weaver BT, Sevensma ET, Haut RC. Chronic changes in rabbit retro-patellar cartilage and subchondral bone after blunt impact loading of the patellofemoral joint. J Orthop Res 2002;20(3):545–50.
24. Wang Y, Wluka AE, Cicuttini FM. The determinants of change in tibial plateau bone area in osteoarthritic knees: a cohort study. Arthritis Res Ther 2005;7(3):R687–93.
25. Wang Y, Wluka AE, Davis S, Cicuttini FM. Factors affecting tibial plateau expansion in healthy women over 2.5 years: a longitudinal study. Osteoarthritis Cartilage 2006;14(12):1258–64.
26. van Osch GJ, van der Kraan PM, van Valburg AA, van den Berg WB. The relation between cartilage damage and osteophyte size in a murine model for osteoarthritis in the knee. Rheumatol Int 1996;16(3):115–9.
27. Pottenger LA, Phillips FM, Draganich LF. The effect of marginal osteophytes on reduction of varus-valgus instability in osteoarthritic knees. Arthritis Rheum 1990;33(6):853–8.
28. Kallman DA, Wigley FM, Scott WW, Hochberg MC, Tobin JD. The longitudinal course of hand osteoarthritis in a male population. Arthritis Rheum 1990;33(9):1323–32.
29. Markhardt BK, Li G, Kijowski R. The clinical significance of osteophytes in compartments of the knee joint with normal articular cartilage. Am J Roentgenol 2018;210(4):W164–71.
30. Neogi T, Nevitt M, Niu J, Sharma L, Roemer F, Guermazi A, *et al*. Subchondral bone attrition may be a reflection of compartment-specific mechanical load: the MOST Study. Ann Rheum Dis 2010;69(5):841–4.
31. Henrotin Y, Pesesse L, Sanchez C. Subchondral bone and osteoarthritis: biological and cellular aspects. Osteoporos Int : A J Establ Res Coop between Eur Found Osteoporos Natl Osteopor Found USA 2012;23(Suppl 8):S847–51.
32. Bellido M, Lugo L, Roman-Blas JA, Castañeda S, Caeiro JR, Dapia S, *et al*. Subchondral bone microstructural damage by increased remodelling aggravates experimental osteoarthritis preceded by osteoporosis. Arthritis Res Ther 2010;12(4):R152–R.
33. Furman BD, Strand J, Hembree WC, Ward BD, Guilak F, Olson SA. Joint degeneration following closed intraarticular fracture in the mouse knee: a model of posttraumatic arthritis. J Orthop Res 2007;25(5):578–92.
34. Dell'Accio F, De Bari C, El Tawil NMF, Barone F, Mitsiadis TA, O'Dowd J, *et al*. Activation of WNT and BMP signaling in adult human articular cartilage following mechanical injury. Arthritis Res Ther 2006;8(5):R139–R.
35. Dell'Accio F, De Bari C, Eltawil NM, Vanhummelen P, Pitzalis C. Identification of the molecular response of articular cartilage to injury, by microarray screening: Wnt-16 expression and signaling after injury and in osteoarthritis. Arthritis Rheum 2008;58(5):1410–21.
36. Gruber J, Vincent TL, Hermansson M, Bolton M, Wait R, Saklatvala J. Induction of interleukin-1 in articular cartilage by explantation and cutting. Arthritis Rheum 2004;50(8):2539–46.
37. Vincent T, Hermansson M, Bolton M, Wait R, Saklatvala J. Basic FGF mediates an immediate response of articular cartilage to mechanical injury. Proc Natl Acad Sci USA 2002;99(12):8259–64.
38. Pelletier JP, Martel-Pelletier J, Abramson SB. Osteoarthritis, an inflammatory disease: potential implication for the selection of new therapeutic targets. Arthritis Rheum 2001;44(6):1237–47.
39. Goldenberg DL, Egan MS, Cohen AS. Inflammatory synovitis in degenerative joint disease. J Rheumatol 1982;9(2):204–9.
40. Haraoui B, Pelletier JP, Cloutier JM, Faure MP, Martel-Pelletier J. Synovial membrane histology and immunopathology in rheumatoid arthritis and osteoarthritis. In vivo effects of antirheumatic drugs. Arthritis Rheum 1991;34(2):153–63.
41. Farahat MN, Yanni G, Poston R, Panayi GS. Cytokine expression in synovial membranes of patients with rheumatoid arthritis and osteoarthritis. Ann Rheum Dis 1993;52(12):870–5.
42. Smith MD, Triantafillou S, Parker A, Youssef PP, Coleman M. Synovial membrane inflammation and cytokine production in patients with early osteoarthritis. J Rheumatol 1997;24(2):365–71.
43. Tindell AG, Kelso EB, Ferrell WR, Lockhart JC, Walsh DA, Dunning L, *et al*. Correlation of protease-activated receptor-2 expression and synovitis in rheumatoid and osteoarthritis. Rheumatol Int 2012;32(10):3077–86.
44. Walsh DA, Yousef A, McWilliams DF, Hill R, Hargin E, Wilson D. Evaluation of a Photographic Chondropathy Score (PCS) for pathological samples in a study of inflammation in tibiofemoral osteoarthritis. Osteoarthritis Cartilage 2009;17(3):304–12.

45. Spector TD, Hart DJ, Nandra D, Doyle DV, Mackillop N, Gallimore JR, *et al*. Low-level increases in serum C-reactive protein are present in early osteoarthritis of the knee and predict progressive disease. Arthritis Rheum 1997;40(4):723–7.
46. Punzi L, Ramonda R, Oliviero F, Sfriso P, Mussap M, Plebani M, *et al*. Value of C reactive protein in the assessment of erosive osteoarthritis of the hand. Ann Rheum Dis 2005;64(6):955–7.
47. Chia S-L, Sawaji Y, Burleigh A, McLean C, Inglis J, Saklatvala J, *et al*. Fibroblast growth factor 2 is an intrinsic chondroprotective agent that suppresses ADAMTS-5 and delays cartilage degradation in murine osteoarthritis. Arthritis Rheum 2009;60(7):2019–27.
48. Ivanavicius SP, Ball AD, Heapy CG, Westwood FR, Murray F, Read SJ. Structural pathology in a rodent model of osteoarthritis is associated with neuropathic pain: increased expression of ATF-3 and pharmacological characterisation. Pain 2007;128(3):272–82.
49. Boegard T, Rudling O, Petersson IF, Jonsson K. Correlation between radiographically diagnosed osteophytes and magnetic resonance detected cartilage defects in the patellofemoral joint. Ann Rheum Dis 1998;57(7):395–400.
50. Sengupta M, Zhang YQ, Niu JB, Guermazi A, Grigorian M, Gale D, *et al*. High signal in knee osteophytes is not associated with knee pain. Osteoarthritis Cartilage 2006;14(5):413–7.
51. Neogi T, Guermazi A, Roemer F, Nevitt MC, Scholz J, Arendt-Nielsen L, *et al*. Association of joint inflammation with pain sensitization in knee osteoarthritis: the multicenter osteoarthritis study. Arthritis Rheumatol 2016;68(3):654–61.